Correspondence between behavioral and individually "optimized" otoacoustic emission estimates of human cochlear input/output curves[a)]

Peter T. Johannesen and Enrique A. Lopez-Poveda[b)]
Unidad de Audición Computacional y Psicoacústica, Instituto de Neurociencias de Castilla y León, Universidad de Salamanca, 37007 Salamanca, Spain

(Received 14 December 2009; revised 10 March 2010; accepted 10 March 2010)

Previous studies have shown a high within-subject correspondence between distortion product otoacoustic emission (DPOAE) input/output (I/O) curves and behaviorally inferred basilar membrane (BM) I/O curves for frequencies above ~2 kHz. For lower frequencies, DPOAE I/O curves contained notches and plateaus that did not have a counterpart in corresponding behavioral curves. It was hypothesized that this might improve by using individualized optimal DPOAE primary levels. Here, data from previous studies are re-analyzed to test this hypothesis by comparing behaviorally inferred BM I/O curves and DPOAE I/O curves measured with well-established group-average primary levels and two individualized primary level rules: one optimized to maximize DPOAE levels and one intended for primaries to evoke comparable BM responses at the f_2 cochlear region. Test frequencies were 0.5, 1, and 4 kHz. Behavioral I/O curves were obtained from temporal (forward) masking curves. Results showed high within-subject correspondence between behavioral and DPOAE I/O curves at 4 kHz only, regardless of the primary level rule. Plateaus and notches were equally common in low-frequency DPOAE I/O curves for individualized and group-average DPOAE primary levels at 0.5 and 1 kHz. Results are discussed in terms of the adequacy of DPOAE I/O curves for inferring individual cochlear nonlinearity characteristics.
 [DOI: 10.1121/1.3377087]

PACS number(s): 43.64.Jb, 43.66.Dc [BLM] Pages: 3602–3613

I. INTRODUCTION

Humans can perceive sounds over a wide range of sound pressure levels (SPLs) most likely thanks to the functioning of the outer hair cells and their effect on the basilar membrane (BM) vibrations (e.g., Oxenham and Bacon 2003). Indeed, the healthy BM is sensitive to very low-level sounds and the magnitude of its response grows compressively with increasing sound level, thus accommodating a range of ~120 dB SPL to a narrower range of physiological responses (e.g., Robles and Ruggero, 2001). The damaged BM, by contrast, shows reduced sensitivity and linearized responses, which likely explains why hearing-impaired listeners show abnormally high thresholds and narrower dynamic ranges (e.g., Moore, 2007).

Despite its importance to hearing, the input/output (I/O) characteristics of the human BM response are not completely understood. Human BM responses cannot be measured directly so indirect techniques are used to infer I/O curves. There exist various methods to infer BM I/O curves from perceptual data (e.g., Lopez-Poveda and Alves-Pinto, 2008; Nelson *et al.*, 2001; Oxenham and Plack, 1997; Plack and Oxenham, 2000). These behavioral methods are reasonably well grounded (e.g., Bacon and Oxenham, 2004; Oxenham and Bacon, 2004). The different methods yield similar within-subject results (Lopez-Poveda and Alves-Pinto, 2008; Nelson *et al.*, 2001; Rosengard *et al.*, 2005) and they are replicable across different measurement sessions. Unfortunately, they are time consuming and require active participation from the listeners and their training. Therefore, they are unsuitable in clinical contexts or for non-cooperative patients (e.g., infants and the elderly).

Distortion product otoacoustic emission (DPOAE) I/O curves are on average broadly similar to BM I/O curves, both for healthy and damaged cochleae (e.g., Dorn *et al.*, 2001; Neely *et al.*, 2009). Their measurement does not require active participation from the listeners and so it has been suggested that DPOAEs could provide a useful alternative to behavioral methods to infer BM I/O curves (e.g., Janssen and Müller, 2008; Johannesen and Lopez-Poveda, 2008; Lopez-Poveda *et al.*, 2009; Müller and Janssen, 2004). Unfortunately, it is still uncertain that DPOAE I/O curves constitute reasonable estimates of BM I/O curves on an *individual* basis (e.g., Johannesen and Lopez-Poveda, 2008; Williams and Bacon, 2005). The long-term goal of the present research is to define DPOAE stimuli and conditions that would allow using DPOAE I/O curves as a reliable alternative to behavioral methods for inferring individualized, frequency-specific BM I/O curves.

In an earlier study (Johannesen and Lopez-Poveda, 2008), we assessed the within-subject correspondence between behaviorally inferred BM I/O curves and DPOAE I/O curves obtained with typical DPOAE parameters (see be-

[a)]Portions of this work were presented in poster form at Acoustics'08 Paris, 29 June–4 July 2008, Paris, France. Abstract published: J. Acoust. Soc. Am. 123, 3854 (2008).

[b)]Author to whom correspondence should be addressed. Electronic mail: ealopezpoveda@usal.es

 0001-4966/2010/127(6)/3602/12/$25.00

low). We observed a reasonably high correspondence only for test frequencies above ~2 kHz. The correspondence was, however, poorer at lower frequencies (0.5 and 1 kHz) because DPOAE I/O curves showed notches and plateaus that did not occur in corresponding behavioral curves. The reason for the notches and plateaus was uncertain. Two explanations were suggested. First, notches and plateaus could be due to the DPOAE fine structure (Gaskill and Brown, 1990), despite our attempts to reduce it by spectral averaging (Kalluri and Shera, 2001). Second, they could be due to our using suboptimal DPOAE stimulus parameters.

The term "fine structure" is used to refer to rapid and local variations present in the graphical representation of $2f_1-f_2$ DPOAE level against test frequency (f_2) (known as the DP-gram). These variations are thought to arise by vector summation of DP contributions generated by various mechanisms from spatially distributed regions within the cochlea, which give rise to peaks and notches in the DP-gram (for a review, see Shera and Guinan, 2008). The same interference mechanism also influences DPOAE I/O curves (He and Schmiedt, 1993, 1997; Mauermann and Kollmeier, 2004).

The fine structure is equally common across test frequencies (Fig. 2 of Mauermann *et al.*, 1999; Fig. 3 of Dhar and Schaffer, 2004), although this evidence is based on rather small sample sizes ($N=4$ and $N=10$, respectively). The notches and plateaus of our I/O curves were, by contrast, present only for low test frequencies. Johnson *et al.* (2006b) reported a higher notch incidence at 2 than at 4 kHz based on a larger subject sample ($N=12-22$), which might be taken as suggestive of greater incidence of plateaus and notches at low frequencies, consistent with the results of our previous study. The evidence of Johnson *et al.* (2006b), however, was based on low primary levels ($L_2=30$ dB SPL), for which the fine structure is known to be more pronounced (He and Schmiedt, 1993, 1997; Mauermann and Kollmeier, 2004; Johnson *et al.*, 2006b). Therefore, it is uncertain that the results of Johnson *et al.* (2006b) may be generalized to 50–60 dB SPL, the range of levels where plateaus and notches were observed in our previous study (Johannesen and Lopez-Poveda, 2008). Furthermore, it is also uncertain that the results of Johnson *et al.* (2006b) can be generalized to 0.5 and 1 kHz, the frequencies where plateaus and notches were more frequent in our data. Additionally, the plateaus and the majority of the notches in the I/O curves of our previous study extended over a wider input level range (approximately 20–30 dB) than that of the notches caused by interference from several DP source contributions [about 10 dB, as estimated from the I/O functions in Figs. 6–8 of He and Schmiedt (1993)]. Lastly, the DPOAE I/O curves reported in our previous study were the mean of several (typically five) I/O curves for adjacent f_2 frequencies in an attempt to reduce the influence of the fine structure by spectral averaging (Kalluri and Shera, 2001). This number was sufficient to account for the fine structure for test frequencies above 2 kHz and so it seems reasonable to assume that it also accounted for the fine structure influence at low frequencies. Altogether, this suggests that the fine structure explanation for the poor correspondence between behavioral and DPOAE I/O curves at low frequencies is possible but may not be sufficient.

Indeed, a complementary explanation may be that the DPOAE I/O curves of our previous study were measured with suboptimal stimulus parameters (Johannesen and Lopez-Poveda, 2008). DPOAE primaries had frequencies (f_1 and f_2) with a ratio of $f_2/f_1=1.2$ (Gaskill and Brown, 1990) and their levels conformed to the rule of Kummer *et al.* (1998): $L_1=39+0.4L_2$, with L_1 and L_2 being the levels of primaries f_1 and f_2, respectively. These parameters were group-average optimal values and were constant across test frequencies; hence it is unlikely that they were optimal on an individual basis. Evidence exists that the primary frequency f_2/f_1 ratio has only a small effect on the shape and slope of I/O curves (Johnson *et al.*, 2006a). By contrast, there is significant evidence that primary levels have a stronger influence on the shape and slope of I/O curves. First, individualized optimal level rules vary significantly across listeners and test frequencies (Neely *et al.*, 2005). Second, only 10% of the subjects have non-monotonic I/O curves in the frequency range from 1 to 8 kHz when using individually optimized DPOAE primary levels (Kummer *et al.*, 2000). Third, numerical simulations shown in Appendix A and elsewhere (Lukashkin and Russell, 2001) suggest that (1) suboptimal primary levels may lead to non-monotonic DP I/O curves, even in the absence of secondary DP sources; and (2) the use of optimal primary levels improves the correspondence between DP I/O curves and I/O curves measured using single tones. Lastly, Lopez-Poveda and Johannesen (2009, 2010) have confirmed that individualized optimal rules for the subjects of their first study (Johannesen and Lopez-Poveda, 2008) differ from the rule of Kummer *et al.* (1998). Altogether this suggests that the correspondence between DPOAE and behaviorally inferred BM I/O curves could improve by using individualized optimal primary levels.

The use of individualized DPOAE optimal levels may also reduce the fine structure. It is known that varying the primary levels can change the relative contribution from the various DP cochlear sources (He and Schmiedt, 1993). To the authors' knowledge, the details are uncertain but one possibility is that individualized optimal primary levels maximize the DPOAE levels by emphasizing the contribution from the "distortion" (f_2) source at the ear canal, which might yield a comparatively smaller "reflection" component and thus reduce the magnitude of the fine structure. If this were the case, then DPOAE I/O curves measured with individualized optimal primary levels may reflect more closely the underlying BM I/O curve at the f_2 cochlear site, and hence improve the match with its corresponding behaviorally inferred I/O curves.

In summary, the fine structure cannot be dismissed as an explanation for the poor correlation between DPOAE and behaviorally inferred BM I/O curves at low frequencies, but the use of individualized DPOAE optimal primary levels would likely improve the correspondence between the results of the two methods.

This study is a re-analysis of previously published data aimed at testing this possibility for a fixed primary frequency

ratio of $f_2/f_1=1.2$. An attempt is made to minimize fine structure effects by averaging DPOAE I/O curves for a number of f_2 frequencies around the test frequency of interest. If successful, such an approach would be more time consuming than DPOAE I/O curve measurement procedures with standard parameters but still advantageous over behavioral methods for estimating individualized, frequency-specific BM I/O curves. Furthermore, it could be put in practice with current advanced DPOAE clinical devices.

II. METHODS

A. Approach

The approach involved within-subject comparisons of DPOAE I/O curves for optimal stimuli with BM I/O curves inferred behaviorally from temporal masking curves (TMCs).

A TMC is a graphical representation of the level of a pure tone forward masker required to just mask a fixed, low-level pure tone probe, as a function of the time interval between the masker and the probe. It is assumed that the slope of a TMC reflects the rate of increase of the BM response to the masker at the BM place tuned to the probe frequency *and* the post-cochlear decay rate of the internal masker effect (Nelson *et al.*, 2001). There is evidence that the latter is approximately constant across masker frequencies and over a wide range of masker levels (Lopez-Poveda and Alves-Pinto, 2008; Wojtczak and Oxenham, 2009). Hence, approximate BM I/O curves may be inferred by plotting the levels of a linear reference TMC (i.e., the TMC for a masker that evokes a linear BM response) against the levels for the TMC for the frequency of interest paired according to time interval (Nelson *et al.*, 2001).

Individualized optimal DPOAE stimuli may be found empirically; that is, by searching combinations of primary frequencies and levels that maximize the level of the $2f_1-f_2$ DPOAE (e.g., Kummer *et al.*, 2000; Johnson *et al.*, 2006a). Optimal stimuli differ across individuals and test frequencies. In the present study, the primary frequency ratio was fixed at $f_2/f_1=1.2$. Therefore, the terms "optimal DPOAE stimuli" and "optimal DPOAE level rule" are used here to refer to the individualized combination of primary levels L_1 and L_2 that evokes the maximal level of the $2f_1-f_2$ DPOAE component for any test frequency f_2.

It has been conjectured that primary levels are optimal when both primaries evoke comparable responses in the f_2 BM region (Kummer *et al.*, 2000). We have recently provided support for this conjecture by comparing empirical optimal levels with levels of equally effective primaries as inferred from TMCs (Lopez-Poveda and Johannesen, 2009). We measured TMCs for two masker frequencies, f_{m1} and f_{m2}, equal to the DPOAE primary frequencies ($f_{m1}=f_1$ and $f_{m2}=f_2$) for a probe frequency (f_P) equal to the DPOAE test frequency ($f_P=f_2$). Based on the TMC interpretation explained above, the levels of two equally effective pure tones were inferred by plotting the levels of the f_{m1} masker, L_{m1}, against those of the f_{m2} masker, L_{m2}, paired according to time interval. The resulting $L_{m1}-L_{m2}$ functions overlapped reasonably well with corresponding plots of empirical DPOAE optimal L_1-L_2 levels for the same subject, thus supporting the conjecture of Kummer *et al.* (2000). The overlap was, however, restricted to L_2 levels below ~65 dB SPL.

Our former reports did not address the main question of the present study but contained a great deal of the data necessary to do it. Therefore, for convenience, the approach here consisted of re-analyzing the data of our earlier reports (Johannesen and Lopez-Poveda, 2008; Lopez-Poveda and Johannesen, 2009, 2010) with the aim of testing if the correspondence between behavioral and DPOAE estimates of BM I/O curves improves when DPOAEs are measured with individualized optimal primary levels. For completeness, the present study extended to DPOAE I/O curves measured using individualized TMC-based primary level rules [from Lopez-Poveda and Johannesen (2009)] and the group-average level rule of Kummer *et al.* (1998). Methodological details have been amply described in the relevant earlier studies (summarized in Appendix B) and only a brief description is provided here.

B. Subjects

Fifteen normal-hearing listeners participated in the study. Their ages ranged from 20 to 39 years. All of them had thresholds within 20 dB hearing level (HL) (ANSI, 1996) at the frequencies considered in this study (0.5, 1, and 4 kHz). They are identified here as in our earlier studies (see Appendix B).

C. TMC stimuli

TMCs were measured for probe frequencies (f_P) of 0.5, 1, and 4 kHz and for masker frequencies (f_2) equal to the f_P. TMCs were also measured for a probe frequency of 4 kHz and a masker frequency of 1.6 kHz. The latter were regarded as the linear reference (Lopez-Poveda and Alves-Pinto, 2008). These TMCs were used to infer BM I/O curves for all probe frequencies (Lopez-Poveda *et al.*, 2003). Additional TMCs were measured for probe frequencies of 0.5, 1, and 4 kHz and for masker frequencies (f_1) equal to $f_P/1.2$. These TMCs, together with those for masker frequencies f_2, were used to infer individualized DPOAE primary rules so that the two primaries evoked equal-BM excitation at the f_2 site (see Secs. II A and II F).

Probe level was fixed at 9 dB sensation level (SL) (i.e., 9 dB above the individual's absolute threshold for the probe).

D. TMC procedure

Masker levels at threshold were measured using a two-interval, two-alternative, forced-choice, procedure. Feedback was provided to the listener. Masker level was changed according to a two-up, one-down adaptive procedure to estimate the 71% point on the psychometric function (Levitt, 1971). The initial step size was 6 dB. The step size was decreased to 2 dB after three reversals. A total of 15 reversals were measured. Threshold was calculated as the mean of the masker levels for the last 12 reversals. A measurement was discarded if the associated standard deviation (SD) exceeded 6 dB. Three threshold estimates were obtained in this way and their mean was taken as the masker level at masked

threshold. If the SD of these three measurements exceeded 6 dB, a fourth threshold estimate was obtained and included in the mean.

Listeners were trained in the forward-masking task for several hours; at first with a higher probe level of 15 dB SL, and later with a probe level of 9 dB SL, until performance became stable.

E. Inferring BM I/O functions from TMCs

BM I/O functions were inferred from TMCs by plotting the masker levels for the linear reference TMC against the levels for a masker equal in frequency to the probe and paired according to masker-probe time interval (Nelson *et al.*, 2001). The linear reference TMCs were fitted (using a least-squares procedure) with a double exponential function and extrapolated to longer masker-probe time intervals to infer BM I/O functions over the wider possible range of levels.

F. Inferring DPOAE primary level rules from TMCs

A least-squares procedure was used to fit TMCs for the f_1 and f_2 maskers with an *ad-hoc* function (see Lopez-Poveda *et al.*, 2005). Individualized DPOAE level rules were then obtained by plotting the fitted levels for the f_1 masker against the fitted levels for the f_2 masker paired according to the masker-probe time intervals (Lopez-Poveda and Johannesen, 2009). Under the assumption that the post-cochlear recovery from masking is independent of masker frequency, and given that the two masker frequencies were equal to the DPOAE primary frequencies, the resulting curves provided the level relationships for two pure tones of frequencies f_1 and f_2 that evoke comparable excitation levels at the f_2 region of the BM (for a full justification, see Lopez-Poveda and Johannesen, 2009). These will be referred to as TMC-based primary levels.

G. DPOAE stimuli

DPOAE I/O curves were obtained by plotting the magnitude (in dB SPL) of the $2f_1-f_2$ DPOAE as a function of the level L_2 of primary tone f_2. I/O curves were obtained for a fixed primary frequency ratio of $f_2/f_1=1.2$ and three different level rules.

- *Individualized optimal levels.* These were obtained by searching the (L_1,L_2) space to find the value of L_1 that produced the highest DPOAE response level for each value of L_2. L_2 was varied in 5-dB steps within the range 35–75 dB SPL. For each fixed L_2, L_1 was varied in 3-dB steps and the individual's optimal value was found.
- *TMC-based levels.* These were derived from the TMCs for maskers f_1 and f_2 as explained in Sec. II F. Recall that with these levels the two primaries are presumed to evoke comparable responses in the f_2 cochlear region (Lopez-Poveda and Johannesen, 2009).
- *The level rule of* Kummer *et al.* (1998)*:* $L_1=0.4L_2+39$, with L_1 and L_2 in dB SPL. This group-average rule was originally designed for $L_2\leq 65$ dB SPL, but here it was extrapolated to $L_2=75$ dB SPL. When this rule was applied, L_2 ranged from 20 to 75 dB SPL in 5-dB steps, except for $f_2=0.5$ kHz for which it ranged from 45 to 75 dB SPL.

DPOAE I/O curves were measured for test frequencies of 0.5, 1, and 4 kHz for all three level rules. Not all rules were applied to all participants. Indeed, at 0.5 kHz, I/O curves for optimal rules were measured for only three participants due to time restrictions.

A spectral averaging approach (e.g., Kalluri and Shera, 2001; Mauermann and Kollmeier, 2004) was used in an attempt to reduce DPOAE I/O variability due to the fine structure. DPOAE I/O curves were measured for five close f_2 frequencies around the text frequency of interest, and the resulting I/O curves were averaged (details may be found in Johannesen and Lopez-Poveda, 2008; Lopez-Poveda and Johannesen, 2009). For instance, the final DPAOE I/O curve at 4 kHz was the mean of five I/O functions for $f_2=3920$, 3960, 4000, 4040, 4080 Hz. When optimal levels rules were considered, the I/O curves of only three adjacent frequencies (e.g., $f_2=3960$, 4000, 4040 Hz) were averaged due to time constraints.

H. DPOAE stimulus calibration and system artifacts

DPOAE primary levels were calibrated with a Zwislocki DB-100 coupler for each pair of primary frequencies (f_1,f_2). No further *in-situ* adjustment of this calibration was applied.

Instrument artifactual DP responses were controlled for by prolonged measurements in a DB-100 Zwislocki coupler and a plastic syringe with a volume of $\sim$1.5 cc. Tests were performed for high L_2 levels ($>$50 dB) and under the same conditions as real ear-canal measurements. Ear-canal measurements were rejected if they were less than 6 dB above the coupler DP response. This is a stricter criterion than commonly used in clinical contexts (for a comprehensive justification, see Johannesen and Lopez-Poveda, 2008).

I. DPOAE procedure

DPOAE measurements were made with an IHS Smart system (with SMARTOAE software version 4.52) equipped with an Etymotic ER-10D probe. During the measurements, subjects sat comfortably in a double-wall sound attenuating chamber and were asked to remain as steady as possible.

The probe fit was checked before and after each measurement session. The probe remained in the subject's ear throughout the whole measurement session to minimize measurement variance from altering the position of the probe in the ear canal. DPOAEs were measured for a fixed measurement time ranging from 10 to 60 s. A DPOAE measurement was considered valid when it was 2 SD above the measurement noise floor (defined as the mean level over ten adjacent frequency bins in the spectrum). When a response did not meet this criterion, the measurement was repeated and the measurement time increased if necessary. The probe remained in the same position during these re-measurements. If the required criterion was not met after successive tries, the measurement point was discarded.

When measuring optimal level rules, system artifacts sometimes occurred for high L_2 levels (70–75 dB SPL) and some of the higher L_1 values. A data point for a certain L_2 level was discarded when an optimal L_1 level could not be found within the range of L_1 levels whose DPOAE responses passed the artifact criterion. In other cases, DPOAE responses passed the artifact criterion for the whole range of L_1 levels but no optimal L_1 value could be found because the instrument limits it to 80 dB SPL. That is, the optimal L_1 would have been almost certainly above 80 dB SPL. In these cases, the true DPOAE response would be higher. These points were noted and included in the correspondence analyses (see below).

J. Analysis of the correspondence between behavioral and DPOAE I/O curves

The degree of within-subject correspondence between BM I/O curves inferred from TMCs and DPOAEs was assessed by least-squares fitting third-order polynomials to all I/O curves (e.g., Johannesen and Lopez-Poveda, 2008). The first derivative of the polynomials was calculated analytically and evaluated for the range of input (behavioral) or L_2 (DPOAEs) levels for which experimental data were available. The similarity between behavioral and DPOAE I/O curves was then assessed by the root mean square (rms) difference between the *slopes* of the behavioral and DPOAE I/O curves *for a corresponding range of input levels*. Considering the difference between the first derivatives instead of the polynomials themselves has the advantage of accounting for the large disparity between behavioral and DPOAE output levels while preserving the information about the shape of the I/O curves. In other words, a first-derivative rms difference of zero indicates I/O curves that may be vertically shifted from each other but are otherwise identical.

Two additional measures were employed to assess the similarity between the degree of BM *compression* suggested by behavioral and DPOAE I/O curves. First, a linear regression (LR) analysis was applied to the minimum value of slope of the third-order polynomials fitted to the I/O curves. Second, a LR analysis was applied to the slope of straight lines fitted by least-squares to I/O curves segments for input (or L_2) levels between 40 and 65 dB SPL. This level range was considered because it typically covered the compressive portion of the I/O curves (Johannesen and Lopez-Poveda, 2008).

These LR analyses were applied to the three sets of DPOAE I/O curves obtained with the three primary levels rules considered in the present study (i.e., optimal, TMC-based, and Kummer).

III. RESULTS

A. TMCs

Except for the linear references of subjects S11–S15, all other TMCs have been reported elsewhere for different purposes. Detailed interpretations of their characteristics can be found in the relevant studies (summarized in Appendix B).

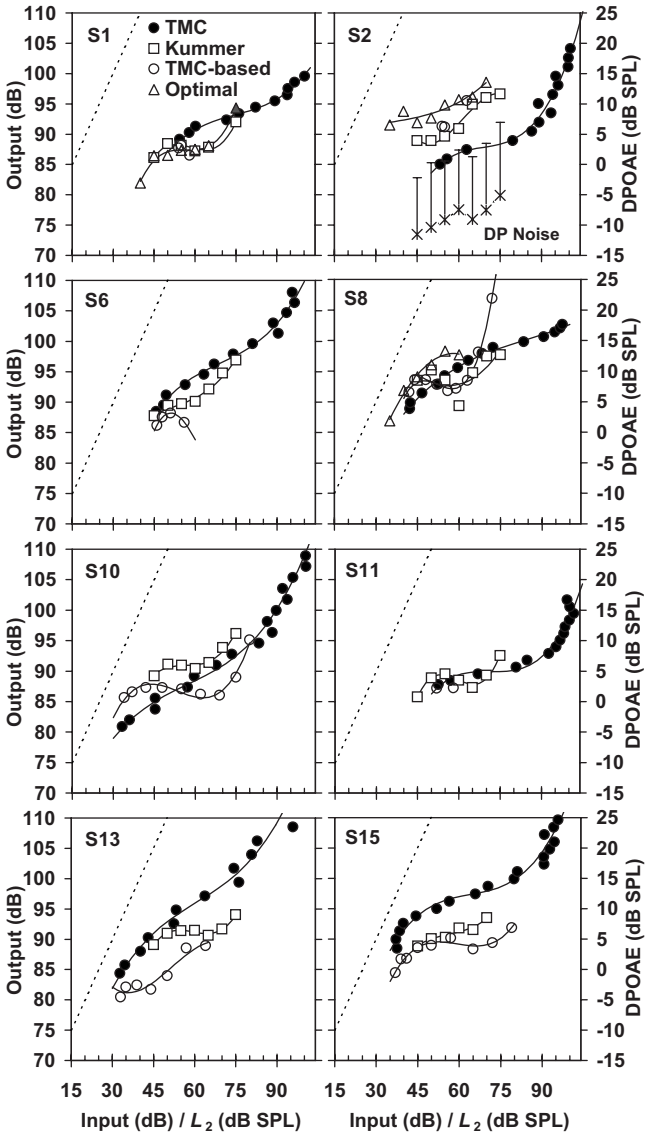

FIG. 1. Behavioral (filled circles) and DPOAE (open symbols) I/O curves at 0.5 kHz for three different primary level rules, as indicated by the inset. Continuous lines illustrate third-order polynomial fits to the experimental points. Each panel illustrates the result for a different participant. The panel for participant S2 also illustrates the mean DP noise floor and its corresponding 2 SDs. Thin dotted lines illustrate a linear response for comparison. Gray symbols illustrate conditions for which primary level L_1 was likely suboptimal because the optimal value would have been higher than the maximum value allowed by the OAE system (80 dB SPL).

B. DPOAE primary level rules

Individualized TMC-based primary level rules were derived from the TMCs for the f_1 and f_2 maskers as described in Sec. II F. Individualized optimal levels were also found as described in Sec. II G. These level rules have been reported and described in great detail elsewhere (see Appendix B).

C. DPOAE I/O curves

Figures 1–3 illustrate DPOAE I/O curves for test frequencies of 0.5, 1, and 4 kHz, respectively. Curves are shown for individualized optimal primary levels (open triangles), individualized TMC-based primary levels (open circles), and the group-average level rule of Kummer *et al.*,

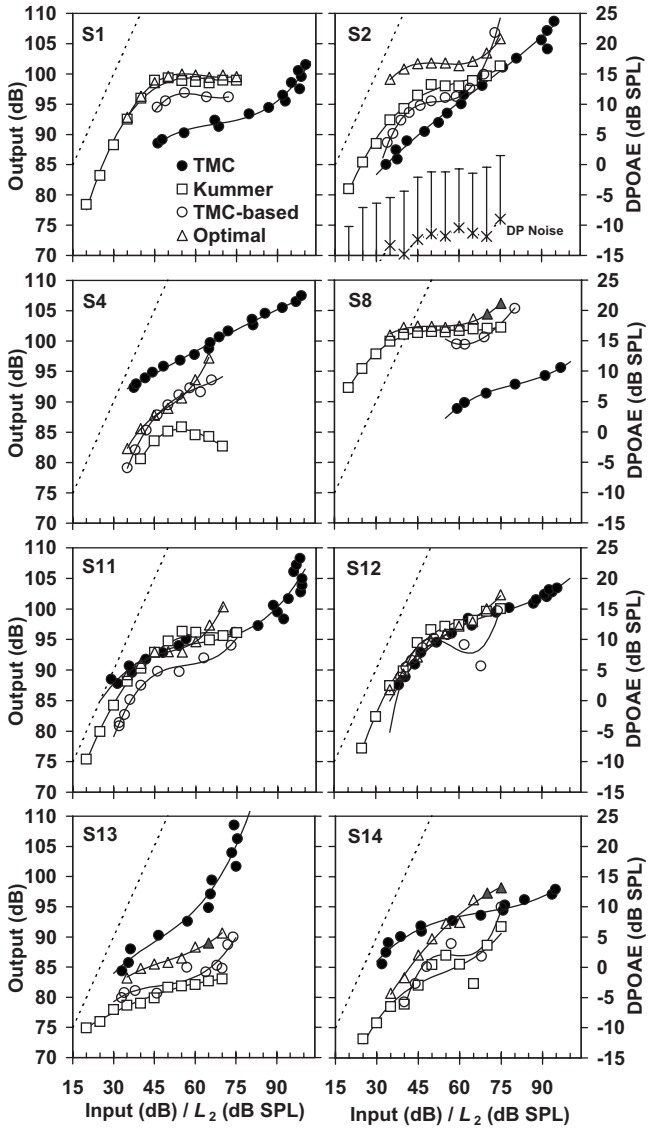

FIG. 2. As Fig. 1 but for a frequency of 1 kHz.

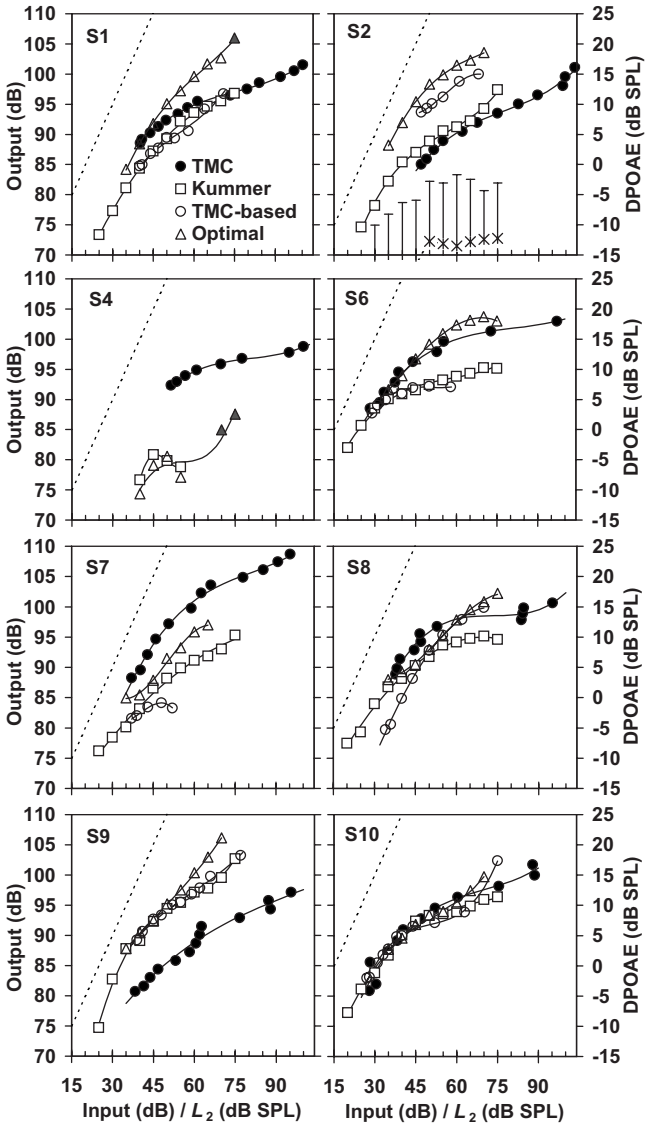

FIG. 3. As Fig. 1 but for a frequency of 4 kHz.

1998 (open squares). Each panel shows the results for a different listener. DPOAE noise levels (crosses) plus two SDs are shown for participant S2 (top-right panels) as a representative example of the noise levels for all other participants. Solid lines illustrate third-order polynomials fitted to the DPOAE I/O curves. Dotted lines illustrate linear responses with a slope of 1 dB/dB. Gray-filled symbols indicate responses whose associated L_1 level could still have been suboptimal (included in fitted curves).

As expected, DPOAE levels for the optimal stimuli were, with very rare exceptions, comparable or higher than DPOAE levels for TMC-based or Kummer stimuli. The very few exceptions (e.g., S11 at 1 kHz and L_2=50 dB SPL in Fig. 2) were possibly due to changes in the position of the probe across DPOAE measurements for the three level rules.

DPOAE I/O curves could be typically (but not always) described as having a steep segment (approaching linearity) at low L_2 levels, followed by a shallower segment at midrange levels. Some curves showed a steeper segment at high L_2 levels that approached linearity. This general trend is characteristic of BM I/O curves (e.g., Robles and Ruggero, 2001). It is noteworthy that the shallower segments of many curves showed plateaus (i.e., regions with a slope of ~0 dB/dB) or notches (i.e., regions with negative slopes), some of which were very sharp. These features were very common at 0.5 (e.g., S1, S6, S8, S10, S11, S13, and S15 in Fig. 1) and 1 kHz (e.g., S1, S2, S8, and S14 in Fig. 2) but virtually nonexistent at 4 kHz. Table I summarizes the number of I/O curves having plateaus or negative-slope segments for each of the three level rules and test frequencies. Rather surprisingly, notches and plateaus occurred at 0.5 and 1 kHz not only for the group-average level rule of Kummer *et al.* (1998) but also for individualized levels, even for optimal levels (e.g., S1, S2, or S8 at 1 kHz).

TABLE I. Incidence of plateaus and notches in DPOAE I/O curves across test frequencies and primary level rules. The numbers between parentheses indicate the total number of I/O curves measured for each condition.

Frequency (kHz)	0.5	1	4
Kummer rule	5 (8)	5 (8)	2 (8)
TMC-based	5 (8)	4 (8)	2 (8)
Optimal	2 (3)	4 (8)	1 (8)

It is interesting to compare the I/O curves obtained with the three primary level rules. At 0.5 kHz (Fig. 1), I/O curves for optimal levels were available for three participants only (S1, S2, and S8) and individualized TMC-based levels often did not cover a sufficient level range to allow a useful comparison. At 1 and 4 kHz (Figs. 2 and 4), where data points were more numerous, visual inspection revealed that I/O curves for the three level rules had reasonably similar shapes (e.g., S1, S8, S11, and S13 at 1 kHz; S1, S2, S7, S9, and S10 at 4 kHz) but with some exceptions (S4 and S14 at 1 kHz; S6 and S8 at 4 kHz). For most of these exceptions, I/O curves for optimal (open triangles) and TMC-based levels (open circles) generally shared many characteristics and they both differed from the curves measured with Kummer's rule (open squares). Optimal levels and to a lesser extent also TMC-based levels tended to produce a rapid increase of DPOAE levels for levels $L_2 > \sim 65$ dB (e.g., S2, S8, and S11 at 1 kHz; S9 and S10 at 4 kHz), although there were exceptions (S1 at 1 kHz; S6 at 4 kHz). Such rapid increases were much rarer for I/O curves measured with Kummer's rule (S2 at 4 kHz).

D. Correspondence between behavioral and DPOAE I/O curves

Behavioral I/O curves (filled circles in Figs. 1–3) showed the same general trend as DPOAE I/O curves, having steep, shallow (compressive), and steep segments at low, moderate, and high input levels, respectively. Unlike for DPOAE I/O curves, however, behavioral I/O curves rarely showed plateaus or notches.

Visual inspection revealed a reasonable correspondence between behavioral and DPOAE I/O curves for the three level rules at 4 kHz (Fig. 3). This was expected for the Kummer rule because the present data had already been reported by Johannesen and Lopez-Poveda (2008). The question is whether the match improved for any of the individualized primary levels (optimal or TMC-based). Optimal levels did improve the correspondence sometimes (e.g., S6 and S7). Other times, however, the correspondence decreased (e.g., S8 and S9). TMC-based levels did not improve the correspondence between DPOAE and behavioral I/O curves.

At 0.5 and 1 kHz (Figs. 1 and 2), however, the correspondence between behavioral and DPOAE I/O curves was disappointing even for DPOAEs measured with individualized optimal or TMC-based levels. With a few exceptions (S11 and S12 at 1 kHz in Fig. 2), behavioral I/O curves were strikingly different from all DPOAE I/O curves. The difference could generally be attributed to the above mentioned plateaus and notches that only occurred for DPOAE I/O curves.

Figure 4 provides quantitative support to the preceding qualitative description. It illustrates rms differences between the slopes of DPOAE and behavioral I/O curves (see Sec. II) against test frequencies, with primary level rules as the parameter (as indicated by the inset). Each open symbol illustrates the rms difference for a given participant. Filled symbols illustrate mean values across participants. Mean differences (filled symbols) were statistically identical across test frequencies and rules. Mean differences tended to be smaller for the Kummer and optimal level rules at 4 kHz than at 0.5 kHz (unpaired t-test, $0.05 < p < 0.10$). Indeed, the mean difference for all three rules tended to decrease with increasing frequency. The *range* of individual differences was comparable for DPOAE I/O curves measured with the rule of Kummer *et al.* (1998) and the optimal rule and they were always narrower than the TMC-based rule.

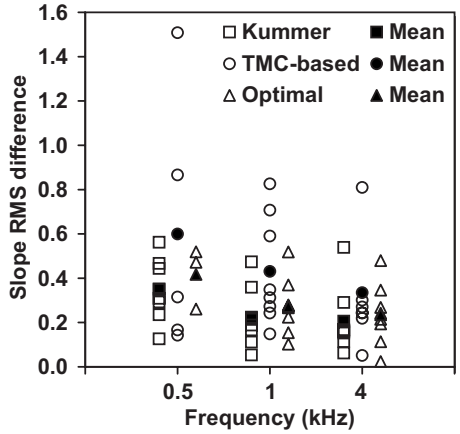

FIG. 4. Root mean square differences between the slope of behavioral and DPOAE I/O curves for different primary level rules, as indicated by the inset. Open and filled symbols illustrate individual and mean values across listeners, respectively.

E. Correspondence of compression estimates

Some authors regard the slope of I/O curves over their nonlinear (compressive) segments as a useful description of the physiological status of the cochlea [reviewed by Robles and Ruggero (2001)]. Others suggest, by contrast, that it does not change with amount of hearing loss (Plack *et al.*, 2004). In any case, given that DPOAE I/O curves sometimes show plateaus and/or notches, which may be absent in their behavioral counterparts, the slope of I/O curves over their compressive segments constitutes a useful variable for assessing their correspondence between behavioral and DPOAE I/O curves. Slopes have been often calculated as the average value over the I/O curve compressive region (e.g., Lopez-Poveda *et al.*, 2003; Plack *et al.*, 2004). Sometimes, however, the slope changes smoothly over the compressive region (e.g., Nelson *et al.*, 2001) and so the minimum, instead of the average, slope is used (e.g., Johannesen and Lopez-Poveda, 2008). Another consideration is that average slope may prove less sensitive to sharp notches, like those present in DPOAE I/O curves. Here, the two descriptors (minimum and average slope values) were considered for assessing the correspondence between DPOAE and behavioral I/O curves over their compressive regions (see Sec. II).

Figure 5 and 6 show, respectively, plots of minimum and average slopes of DPOAE I/O curves against corresponding slopes for behavioral curves. Each panel is for a different test frequency. Each point illustrates results for a single participant. Different symbols illustrate results for DPOAEs measured with different levels rules, as indicated by the inset in the top panels. Thick lines illustrate LR functions fitted by least-squares to the experimental data points, as indicated by the inset. The diagonal represents perfect correspondence (il-

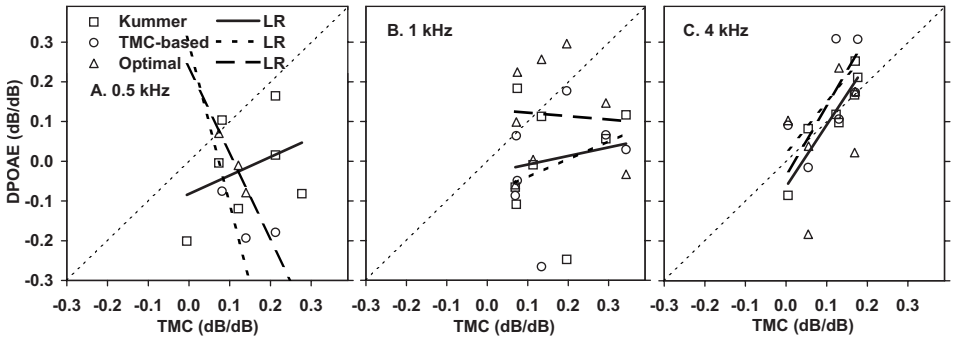

FIG. 5. Correspondence between minimum compression-exponent estimates obtained from third-order polynomials fitted to behavioral and DPOAE I/O curves at 0.5, 1, and 4 kHz. Each point represents data for one subject and one level rule, as indicated by the inset in panel (A). Thick lines show LR fits to the data points for each of the stimulus rules. Diagonal thin dotted lines illustrate perfect correspondence.

lustrated by thin dotted lines). Tables II and III summarize the results of LR analysis on these compression estimates. The correspondence can be regarded as good when the LR slope (a) and intercept (b) are close to one and zero, respectively, and the F-statistics allow rejecting the null-hypothesis (there is no statistical association between the two data sets).

Correspondence between DPOAE and behavioral compression estimates was clearly poor at 0.5 and 1 kHz regardless of the compression descriptor (i.e., minimum or average slope) or the level rule used to measure DPOAEs. For both compression descriptors (Tables II and III), the linear regression slope and intercept were far from 1 and 0.

At 4 kHz, reasonably high correspondence was observed for the minimum slope estimate (Fig. 5) for DPOAEs measured with the Kummer rule (slope=1.55; intercept=−0.06; r^2=0.86; $p<0.01$). Correspondence was lower for individualized level rules and was not significant (Table II). For the average slope estimates (Fig. 6), there was moderate correspondence for DPOAEs measured with the Kummer rule and the optimal rule, but it did not reach significance (both p =0.11). The two individualized rules (optimal and TMC-based) yielded reasonably similar minimum compression estimates (slope=1.72; intercept=−0.08; r^2=0.89; $p<0.005$; data not shown). This is not surprising given that both individualized rules were very similar, presumably because they reflect levels of equally effective primaries at the f_2 cochlear site (Lopez-Poveda and Johannesen, 2009).

IV. DISCUSSION

The long-term goal of the present research is to define DPOAE stimuli and conditions that would allow using DPOAEs as a universal and faster alternative to behavioral methods to infer individualized, frequency-specific BM I/O curves. Previous studies have shown that this is possible using typical DPOAE stimuli (specifically, the rule of Kummer *et al.*, 1998 and a frequency ratio of f_2/f_1=1.2) for test frequencies above ~2 kHz but not for lower frequencies (Johannesen and Lopez-Poveda, 2008). The main reason for the lack of correspondence at these lower frequencies seemed to be the presence of notches and plateaus in DPOAE I/O curves that did not have a counterpart in behavioral curves. The present study aimed at testing whether the correspondence between the I/O curves inferred with the two methods would improve by using DPOAE individualized optimal primary levels. Two individualized level rules have been considered: one optimized to maximize DPOAE levels and one intended for primaries to evoke comparable BM responses at the f_2 cochlear site. It has been shown that this approach does not improve the correspondence between behavioral and DPOAE I/O curves at low frequencies with respect to the group-average levels of Kummer *et al.* (1998). Indeed, it has been shown that plateaus and notches are equally common in DPOAE I/O curves for individualized and group-average DPOAE primary levels at 0.5 and 1 kHz (Table I).

The similar morphology of DPOAE I/O curves measured with different primary levels (Figs. 1–3) suggests a lower dependency on individualized levels than expected (see Introduction and Appendix A). For example, all DPOAE I/O curves suggested similar compression thresholds, as well as similar slopes below and above the compression threshold (Fig. 1–3). This was true for most participants (the only exceptions were S4 at 1 kHz, and S6 and S8 at 4 kHz). How-

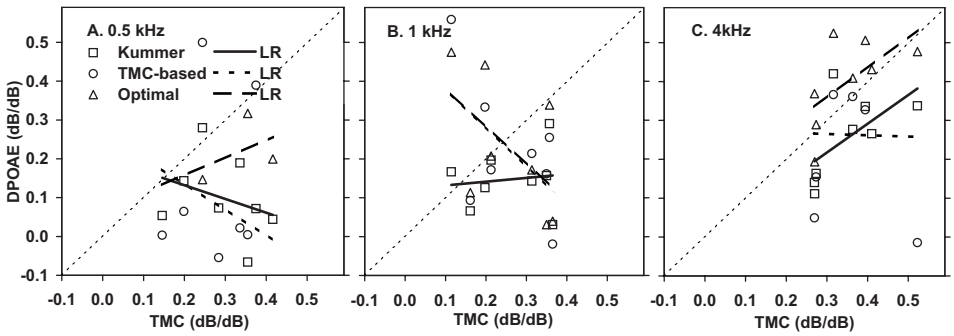

FIG. 6. As Fig. 5 but for the average slope of behavioral and DPOAE I/O curves over their compressive region (input levels from 40 to 65 dB SPL).

TABLE II. Results of linear regression analysis between the minimum slopes of third-order polynomials fitted to behavioral and DPOAE I/O curves for the three level rules. *a*: slope; *b*: intercept; r^2: predicted variance; *N*: number of data points; *p*=probability of observed regression occurring by chance (i.e., $p<0.05$ indicates a statistically significant regression); n.a.: not applicable (LR statistics were not calculated if $N<4$).

Frequency (kHz)			0.5		
Level rule	*a*	*b*	r^2	*N*	*p*
Kummer	0.47	−0.08	0.13	7	0.42
TMC-based	−3.99	0.29	0.38	4	0.39
Optimal	n.a.	n.a.	n.a.	3	n.a.
Frequency (kHz)			1		
Level rule	*a*	*b*	r^2	*N*	*P*
Kummer	0.22	−0.03	0.03	8	0.70
TMC-based	0.45	−0.09	0.13	7	0.43
Optimal	−0.09	0.13	0.00	8	0.87
Frequency (kHz)			4		
Level rule	*a*	*b*	r^2	*N*	*P*
Kummer	1.55	−0.06	0.86	7	0.0025
TMC-based	1.25	0.02	0.43	6	0.16
Optimal	1.72	−0.03	0.27	8	0.18

ever, the tendency to a rapid increase in the DPOAE response at high levels ($L_2 > \sim 70$ dB SPL) seemed peculiar to individualized (optimal and TMC-based) levels. Such a tendency was rarely observed in I/O curves measured with the rule of Kummer *et al.* (1998). The slight influence of the level rule on slope may also explain the rather surprising result that the match between behavioral and DPOAE I/O curves was closest for the Kummer rule even though it is a group-average estimate that disregards individual idiosyncrasies. Despite their modest influence on the shape of DPOAE I/O curves, individualized primary levels may nevertheless be important to maximize the DPOAE absolute levels, and thus to maximize the sensitivity of DPOAEs as a potential clinical diagnostic tool (Kummer *et al.*, 2000).

TABLE III. As Table II, but for linear regression analysis between the slopes of straight lines fitted to the compressive segments of behavioral and DPOAE I/O curves (Fig. 6).

Frequency (kHz)			0.5		
Level rule	*a*	*b*	r^2	*N*	*P*
Kummer	−0.35	0.20	0.10	8	0.45
TMC-based	−0.67	0.27	0.06	8	0.57
Optimal	n.a.	n.a.	n.a.	3	n.a.
Frequency (kHz)			1		
Level rule	*a*	*b*	r^2	*N*	*P*
Kummer	0.10	0.12	0.01	8	0.78
TMC-based	−1.01	0.48	0.33	8	0.13
Optimal	−0.97	0.48	0.31	8	0.15
Frequency (kHz)			4		
Level rule	*a*	*b*	r^2	*N*	*P*
Kummer	0.74	0.00	0.36	8	0.11
TMC-based	−0.03	0.28	0.00	7	0.98
Optimal	0.78	0.12	0.38	8	0.11

A. The causes of low-frequency plateaus of notches

It has been shown that plateaus and notches are equally common in DPOAE I/O curves for individualized and group-average DPOAE primary levels at 0.5 and 1 kHz (Table I). The present study was not intended to provide an explanation for the low-frequency notches and plateaus, but the present results, in combination with existing evidence, provide interesting insights. As argued in the Introduction, plateaus and notches could be due to the fine structure and the use of suboptimal DPOAE stimuli. Further, it was conjectured that these two explanations need not be independent of each other in so far as the fine structure changes with changing primary levels (He and Schmiedt, 1993).

Regarding the suboptimal parameter explanation, a fixed primary frequency ratio of $f_2/f_1=1.2$ has been used in the present study based on early evidence that it maximizes (on average) DPOAE levels (Gaskill and Brown, 1990). According to more recent reports, however, the optimal f_2/f_1 ratio increases slightly with decreasing f_2 frequency and with increasing L_2 level (Johnson *et al.*, 2006a), particularly for low frequencies. To the best of the authors' knowledge, the optimal ratio for a test frequency of 0.5 kHz is yet to be determined. There is evidence, however, that human cochlear processing in apical BM regions may be significantly different from that of basal zones (e.g., Lopez-Poveda *et al.*, 2003; Plack *et al.*, 2004), which suggests that the optimal frequency ratio at 0.5 kHz likely differs from 1.2. Therefore, a better correspondence between behavioral and DPOAE I/O curves might have been obtained by considering not only optimal primary levels but also optimal primary frequencies. On the other hand, variations of the f_2/f_1 ratio seem to have only a small effect on the slope of average I/O curves below 65 dB SPL (e.g., Fig. 3 of Johnson *et al.*, 2006a), at least in the frequency range from 1 to 8 kHz. This casts doubts that optimizing the frequency ratio would improve the correspondence between behavioral and DPOAE I/O curves, but the benefit it could have on an individual basis is yet to be investigated.

Regarding the fine structure explanation, arguments have been given in the Introduction to suggest that this explanation is possible but may not be sufficient. The arguments provided were based on existing evidence for test frequencies equal to or greater than 2 kHz. The importance of the fine structure for frequencies below 1 kHz is still uncertain but the present results suggest that it could more significant than was thought at the outset of the present study. If this were the case, it would explain why the spectral averaging method employed here to minimize the fine structure seemed more efficient for high (4 kHz) than for low (0.5 and 1 kHz) test frequencies. The reason for this is uncertain. If the interference between the DP contributions from various cochlear regions (Shera and Guinan, 2008) was more pronounced and less sensitive to primary levels and f_2 frequencies for low than for high-frequency DPOAEs, this might explain the relatively higher incidence of plateaus and notches at low frequencies and for all level rules considered. By extension, it might also explain the observed discrepancies between behavioral and DPOAE I/O curves. It is uncer-

tain why destructive interference would be more pronounced or less sensitive to primary levels at low than at high frequencies. Interestingly, however, both outer hair cell disorganization (e.g., Lonsbury-Martin *et al.*, 1988) and compression bandwidth appear comparatively greater for apical than for basal cochlear regions (e.g., Rhode and Cooper, 1996; Lopez-Poveda *et al.*, 2003; Plack and Drga, 2003). As a result, the generation region of DPOAEs by both "reflection" and "distortion" mechanisms is likely broader in the apex than in the base and hence potential interactions between DPOAE contributions from adjacent regions could be more significant for low test frequencies. This, however, is only a conjecture, whose detailed formulation and verification remain to be developed.

The present data do not support the relationship between the two explanations (fine structure and suboptimal parameters) that has been conjectured in the Introduction. In principle, varying DPOAE primary levels could change the relative contribution from the various DP sources (as measured in the ear canal) and hence the magnitude of the fine structure. It was hypothesized in the Introduction that individualized primary levels could maximize DPOAE levels by emphasizing the contribution from the "distortion" (f_2) source relative to that of the "reflection" ($2f_1-f_2$) source, which would contribute to reduce the fine structure magnitude. The present results show that the incidence and magnitude of notches and plateaus is not reduced by using individualized optimal primary levels and so they do not support the conjecture in question. If anything, the present data would suggest that the magnitude of the contributions from the "reflection" ($2f_1-f_2$) source is proportional to that of the "distortion" (f_2) source.

B. Remarks

The TMC method of inferring behavioral BM I/O relies on several assumptions (see Sec. II and the Discussion of Johannesen and Lopez-Poveda, 2008). The majority of them have received experimental support for a wide range of conditions (e.g., Lopez-Poveda and Johannesen, 2009; Lopez-Poveda and Alves-Pinto, 2008; Wojtczak and Oxenham, 2009). Nevertheless, behavioral curves cannot be taken as an undisputed "golden standard" (e.g., Stainsby and Moore, 2006; Wojtczak and Oxenham, 2009), particularly at low frequencies where there is a lack of correspondence between behavioral and DPOAE I/O curves. In other words, it remains unclear which of the two sets of I/O curves, behavioral or DPOAEs, best represents the underlying BM I/O curves at 0.5 and 1 kHz.

V. CONCLUSIONS

For a fixed primary frequency ratio of $f_2/f_1=1.2$, DPOAE levels vary moderately depending on primary level rule but the fundamental morphology of DPOAE I/O curves hardly changes.

The incidence of plateaus and notches in DPOAE I/O curves was comparable for individualized primary level rules and for the group-average rule of Kummer *et al.* (1998). These features were more frequent at low (0.5 and 1 kHz) than at high (4 kHz) frequencies and remain the most likely reason for the low correspondence between behavioral and DPOAE I/O curves at low frequencies.

The correspondence between behavioral and DPOAE I/O curves was reasonably high at 4 kHz. The group-average primary level rule of Kummer *et al.* (1998) is sufficient to estimate individualized BM I/O curves at high frequencies.

It is uncertain which of two approaches (DPOAEs or behavioral methods) is more appropriate to infer individualized BM I/O responses at 0.5 and 1 kHz, but DPOAEs may *not* be used as an alternative to behavioral methods, even considering individualized optimal primary levels.

ACKNOWLEDGMENTS

We thank the associate editor and two anonymous reviewers for their suggestions to improve the quality of the paper. Work supported by the Spanish Ministry of Science and Innovation (PROFIT CIT-390000-2005-4 and BFU-2006-07536), the Junta de Castilla y León (GR221) and the William Demant Oticon Foundation.

APPENDIX A

In the present study, as in many previous ones (e.g., Dorn *et al.*, 2001; Williams and Bacon, 2005; Johannesen and Lopez-Poveda, 2008; Neely *et al.*, 2009), it is implicitly assumed that the I/O curve for the $2f_1-f_2$ DPOAE would be a reasonable description of a BM site's I/O curve (as measured using pure tones at the site's characteristic frequency-CF) for a site with CF$\sim f_2$. In other words, that it would be possible to infer on-CF BM I/O curves by measuring the growth of the $2f_1-f_2$ DPOAE component with increasing L_2, for f_2=CF. This section provides evidence that this assumption stands a better chance of being reasonable when optimal L_1 levels are considered. Evidence is also shown that suboptimal L_1 levels may produce non-monotonic $2f_1-f_2$ DP I/O curves even in the absence of secondary DP sources (fine structure).

Ideally, the assumption in question should be demonstrated in analytical mathematical form for the nonlinearity underlying BM responses. This, however, is not possible because nonlinear systems do not have exact analytic transfer functions and because the actual form of the BM nonlinearity is, to the authors' knowledge, yet to be confirmed. The present section provides only a crude numerical demonstration of the claims made in the preceding paragraph for two kinds of time-invariant compressive nonlinearities: a broken-stick nonlinear (Meddis *et al.*, 2001) and a double-Boltzmann gain function (e.g., Lukashkin and Russell, 1998, 2001). These nonlinearities have been successfully used to account for BM and outer hair cell responses in computational models. For simplicity, no concurrent filtering effects are considered here.

Let $x(t)$ and $y(t)$ be the time-domain input and output waveforms to/from the nonlinearity. The broken-stick nonlinearity has the form

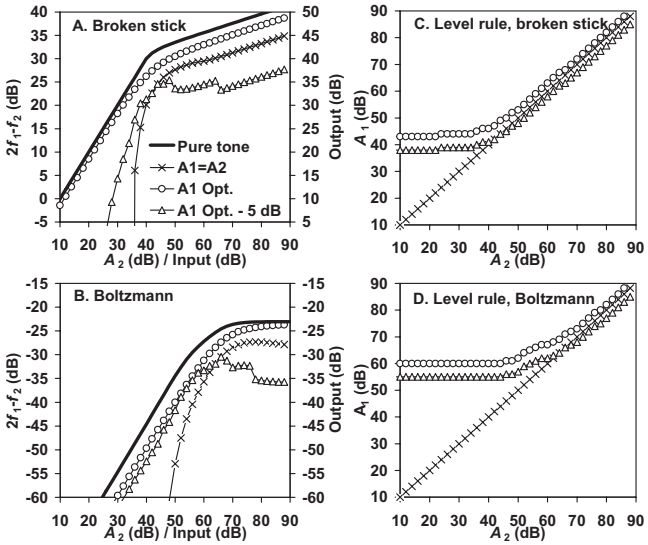

FIG. 7. Simulated I/O curves (left panels) for different amplitude rules (right panels) and two non-linearities: a broken stick (upper panels) and a Boltzmann function (lower panels). [(A) and (B)] Bold continuous lines illustrate I/O curves based on single-sinusoid inputs. Symbols illustrate I/O curves for the $2f_1-f_2$ DP for three different amplitude rules: $A_1=A_2$, A_1 =optimal, and $A_1=A_1$ optimal −5 dB (as indicated in the inset). [(C) and (D)] A_1-A_2 amplitude rules corresponding to the I/O curves of (A) and (B).

$$y(t) = \min[ax(t), bx^c(t)], \tag{A1}$$

where a and b are gain parameters and c is the compression exponent. Likewise, the double-Boltzmann nonlinearity has the form

$$y(t) = G_M\left\{1 + \exp\left(\frac{x_1 - x(t)}{s_1}\right)\left[1 + \exp\left(\frac{x_2 - x(t)}{s_2}\right)\right]\right\}^{-1}, \tag{A2}$$

where G_M, x_1, x_2, s_1, and s_2 are parameters. Here, the input was arbitrarily assumed in units of μPa and the parameters of the two functions were set to the following arbitrary values: $a=1$, $b=437$, $c=0.2$, $G_M=7$, $x_1=41$, $x_2=24$, $s_1=62.5$, and $s_2=15.38$.

The I/O response characteristics of these two nonlinearities were obtained considering one- and two-sinusoid digital input waveforms (sampling frequency=48 kHz). These will be referred to as pure tone (PT) and DP I/O curves, respectively. PT I/O curves were obtained using single sinusoids of a fixed frequency (f_2) and amplitudes (A_2) that varied from 20 to 20×10^5 μPa in steps of 2 dB. A fast Fourier transform (FFT) was applied to the output waveforms and the amplitude at the f_2 frequency was noted and plotted as a function of A_2 in a log-log scale to obtain the I/O curve. DP I/O curves were obtained presenting two simultaneous sinusoids of frequencies f_2 and $f_1=f_2/1.2$. The amplitude of the f_2 sinusoid, A_2, was the same as in the one-sinusoid evaluations. For each value of A_2, the amplitude of the f_1 sinusoid, A_1, varied in 1-dB steps. A FFT was applied to the output waveform and the amplitude of the $2f_1-f_2$ (DP) frequency component was noted.

The top and bottom panels of Fig. 7 illustrate the results for the broken-stick and Boltzmann nonlinearity, respectively. The left and right panels illustrate I/O curves and A_1-A_2 amplitude rules, respectively. PT I/O curves are shown as bold continuous lines. DP I/O curves are shown for three A_1-A_2 combinations: equal-amplitude primaries ($A_1=A_2$) (crosses), optimal A_1 (circles), and A_1 5 dB lower than optimal (triangles). Optimal A_1 are defined here as the A_1 amplitudes that produced the highest DP amplitudes for each value of A_2.

Simple visual inspection to the I/O curves of Fig. 7 reveals that PT I/O curves are most similar to DP I/O obtained with optimal A_1 amplitudes. The figure also reveals that suboptimal A_1 amplitudes can produce non-monotonic DP I/O curves (e.g., triangles). Furthermore, the broken-stick nonlinearity DP I/O curve obtained with slightly suboptimal A_1 amplitudes shows shallow notches. These results are consistent with those of Lukashkin and Russell (2001) and support the claims made at the beginning of this section.

Several things are to be noted. First, the present results do not imply that the maximal correspondence between DP and PT I/O occurs for optimal primary amplitudes; they show that optimal primary amplitudes lead to a reasonable correspondence between DP and PT I/O curves. This result is useful in practice because the A_1-A_2 combination that maximizes the correspondence between the two I/O curves will typically be unknown *a priori*. Second, the main conclusions of this exercise are independent of the nonlinearity parameter values. Third, the present models are very simplistic and do not consider concurrent filtering. For this reason, the present simulations do not depend on the actual frequency of the sinusoids or the parameters of the nonlinearities. Filtering, however, would almost certainly produce different optimal amplitude combinations than those illustrated in Figs. 7(C) and 7(D).

Despite its being an oversimplification, this modeling exercise demonstrates that (1) primary levels strongly influence the shape of the DP I/O curve; (2) suboptimal levels can produce non-monotonic DP I/O curves with plateaus and wide, shallow notches; and (3) the use of optimal levels may enhance the similarity between PT and DP I/O curves.

APPENDIX B

The original data can be found in the following references: the absolute thresholds for the maskers and the probes in Lopez-Poveda and Johannesen (2009); linear reference ($f_m=0.4f_p$) and on-frequency TMCs ($f_m=f_p$) for subjects S1–S10 in Johannesen and Lopez-Poveda (2008); the linear reference TMCs for subjects S11–S15 have not been published before. On-frequency TMCs ($f_m=f_p$) for subjects S11–S15 were taken from Lopez-Poveda and Johannesen (2009). Behavioral I/O curves have been published before for subjects S1–S10 only and are reproduced here for completeness (Figs. 1–3). The TMCs for masker frequencies equal to DPOAE primary frequencies f_1 and f_2 ($f_2=f_P$ and $f_1=f_p/1.2$, respectively) were taken from Lopez-Poveda and Johannesen (2009), and were used to infer TMC-based DPOAE level rules.

DPOAE I/O curves measured with the rule of Kummer *et al.* (1998) can be found in Johannesen and Lopez-Poveda (2008); TMC-based DPOAE primary level rules in Lopez-Poveda and Johannesen (2009); individualized optimal pri-

mary level rules for 1 and 4 kHz in Lopez-Poveda and Johannesen (2009); and individualized optimal primary level rules for 0.5 kHz in Lopez-Poveda and Johannesen (2010). In the case of TMC-based and individualized optimal rules, only *mean* DPOAE I/O curves have been published previously (Lopez-Poveda and Johannesen, 2009).

ANSI (**1996**). *S3.6 Specification for Audiometers* (American National Standards Institute, New York).

Bacon, S. P., and Oxenham, A. J. (**2004**). "Psychophysical manifestations of compression: Normal-hearing listeners," in *Compression. From Cochlea to Cochlear Implants*, edited by S. P. Bacon, R. R. Fay, and A. N. Popper (Springer, New York), Chap. 3, pp. 107–152.

Dhar, S., and Schaffer, L. A. (**2004**). "Effects of a suppressor tone on distortion product otoacoustic emissions fine structure: Why a universal suppressor level is not a practical solution to obtaining single-generator DP-grams," Ear Hear. **25**, 573–585.

Dorn, P. A., Konrad-Martin, D., Neely, S. T., Keefe, D. H., Cyr, E., and Gorga, M. P. (**2001**). "Distortion product otoacoustic emission input/output functions in normal-hearing and hearing-impaired human ears," J. Acoust. Soc. Am. **110**, 3119–3131.

Gaskill, S. A., and Brown, A. M. (**1990**). "The behavior of the acoustic distortion product, 2*f*1-*f*2, from the human ear and its relation to auditory sensitivity," J. Acoust. Soc. Am. **88**, 821–839.

He, N.-J., and Schmiedt, R. A. (**1993**). "Fine structure of the $2f_1$-f_2 acoustic distortion product: Changes with primary level," J. Acoust. Soc. Am. **94**, 2659–2669.

He, N.-J., and Schmiedt, R. A. (**1997**). "Fine structure of the $2f_1$-f_2 acoustic distortion product: Effects of primary level and frequency ratios," J. Acoust. Soc. Am. **101**, 3554–3565.

Janssen, T., and Müller, J. (**2008**). "Otoacoustic emissions as a diagnostic tool in a clinical context," in *Active Processes and Otoacoustic Emissions*, edited by G. A. Manley, R. R. Fay, and A. N. Popper (Springer, New York), Chap. 13, pp. 421–460.

Johannesen, P. T., and Lopez-Poveda, E. A. (**2008**). "Cochlear nonlinearity in normal-hearing subjects as inferred psychophysically and from distortion product otoacoustic emissions," J. Acoust. Soc. Am. **124**, 2149–2163.

Johnson, T. A., Neely, S. T., Garner, C. A., and Gorga, M. P. (**2006a**). "Influence of primary-level and primary-frequency ratios on human distortion product otoacoustic emissions," J. Acoust. Soc. Am. **119**, 418–428.

Johnson, T. A., Neely, S. T., Kopun, J. G., and Gorga, M. P. (**2006b**). "Reducing reflected contributions to ear-canal distortion product otoacoustic emissions in humans," J. Acoust. Soc. Am. **119**, 3896–3907.

Kalluri, R., and Shera, C. A. (**2001**). "Distortion-product source unmixing: A test of the two-mechanism model for DPOAE generation," J. Acoust. Soc. Am. **109**, 622–637.

Kummer, P., Janssen, T., and Arnold, W. (**1998**). "The level and growth behavior of the 2*f*1-*f*2 distortion product otoacoustic emission and its relationship to auditory sensitivity in normal hearing and cochlear hearing loss," J. Acoust. Soc. Am. **103**, 3431–3444.

Kummer, P., Janssen, T., Hulin, P., and Arnold, W. (**2000**). "Optimal L1-L2 primary tone level separation remains independent of test frequency in humans," Hear. Res. **146**, 47–56.

Levitt, H. (**1971**). "Transformed up-down methods in psychoacoustics," J. Acoust. Soc. Am. **49**, 467–477.

Lonsbury-Martin, B. L., Martin, G. K., Probst, R., and Coats, A. C. (**1988**). "Spontaneous otoacoustic emissions in nonhuman primate. II. Cochlear anatomy," Hear. Res. **33**, 69–93.

Lopez-Poveda, E. A., and Alves-Pinto, A. (**2008**). "A variant temporal-masking-curve method for inferring peripheral auditory compression," J. Acoust. Soc. Am. **123**, 1544–1554.

Lopez-Poveda, E. A., Johannesen, P. T., and Merchán, M. A. (**2009**). "Estimation of the degree of inner and outer hair cell dysfunction from distortion product otoacoustic emission input/output functions," Audiological Med. **7**, 22–28.

Lopez-Poveda, E. A., and Johannesen, P. T. (**2009**). "Otoacoustic emission theories and behavioral estimates of human basilar membrane motion are mutually consistent," J. Assoc. Res. Otolaryngol. **10**, 511–523.

Lopez-Poveda, E. A., and Johannesen, P. T. (**2010**). "Otoacoustic emission theories can be tested with behavioral methods," in *The Neurophysiological Bases of Auditory Perception*, edited by E. A. Lopez-Poveda, R. Meddis, and A. R. Palmer (Springer, New York), pp. 3–14.

Lopez-Poveda, E. A., Plack, C. J., Meddis, R., and Blanco, J. L. (**2005**). "Cochlear compression in listeners with moderate sensorineural hearing loss," Hear. Res. **205**, 172–183.

Lopez-Poveda, E. A., Plack, C. J., and Meddis, R. (**2003**). "Cochlear nonlinearity between 500 and 8000 Hz in listeners with normal hearing," J. Acoust. Soc. Am. **113**, 951–960.

Lukashkin, A. N., and Russell, I. J. (**1998**). "A descriptive model of the receptor potential nonlinearities generated by the hair cell mechanoelectrical transducer," J. Acoust. Soc. Am. **103**, 973–980.

Lukashkin, A. N., and Russell, I. J. (**2001**). "Origin of the bell-like dependence of the DPOAE amplitude on primary frequency ratio," J. Acoust. Soc. Am. **110**, 3097–3106.

Mauermann, M., Uppenkamp, S., van Hengel, P. W., and Kollmeier, B. (**1999**). "Evidence for the distortion product frequency place as a source of distortion product emission (DPOAE) fine structure in humans. I. Fine structure and higher-order DPOAE as a function of the frequency ratio *f*2/*f*1," J. Acoust. Soc. Am. **106**, 3473–3483.

Mauermann, M., and Kollmeier, B. (**2004**). "Distortion product otoacoustic emission (DPOAE) input/output functions and the influence of the second DPOAE source," J. Acoust. Soc. Am. **116**, 2199–2212.

Meddis, R., O'Mard, L. P., and Lopez-Poveda, E. A. (**2001**). "A computational algorithm for computing nonlinear auditory frequency selectivity," J. Acoust. Soc. Am. **109**, 2852–2861.

Moore, B. C. J. (**2007**). *Cochlear Hearing Loss*, 2nd ed. (Wiley, Chichester, UK).

Müller, J., and Janssen, T. (**2004**). "Similarity in loudness and distortion product otoacoustic emission input/output functions: Implications for an objective hearing aid adjustment," J. Acoust. Soc. Am. **115**, 3081–3091.

Neely, S. T., Johnson, T. A., and Gorga, M. P. (**2005**). "Distortion-product otoacoustic emission measured with continuously varying stimulus level," J. Acoust. Soc. Am. **117**, 1248–1259.

Neely, S. T., Johnson, T. A., Kopun, J., Dierking, D. M., and Gorga, M. P. (**2009**). "Distortion-product otoacoustic emission input/output characteristics in normal-hearing and hearing-impaired human ears," J. Acoust. Soc. Am. **126**, 728–738.

Nelson, D. A., Schroder, A. C., and Wojtczak, M. (**2001**). "A new procedure for measuring peripheral compression in normal-hearing and hearing-impaired listeners," J. Acoust. Soc. Am. **110**, 2045–2064.

Oxenham, A. J., and Bacon, S. P. (**2003**). "Cochlear compression, perceptual measures and implications for normal and impaired hearing," Ear Hear. **24**, 352–366.

Oxenham, A. J., and Bacon, S. P. (**2004**). "Psychophysical manifestations of compression: Hearing-impaired listeners," in *Compression. From Cochlea to Cochlear Implants*, edited by S. P. Bacon, R. R. Fay, and A. N. Popper (Springer, New York), Chap. 4, pp. 62–106.

Oxenham, A. J., and Plack, C. J. (**1997**). "A behavioral measure of basilar-membrane nonlinearity in listeners with normal and impaired hearing," J. Acoust. Soc. Am. **101**, 3666–3675.

Plack, C. J., and Drga, V. (**2003**). "Psychophysical evidence for auditory compression at low characteristic frequencies," J. Acoust. Soc. Am. **113**, 1574–1586.

Plack, C. J., and Oxenham, A. J. (**2000**). "Basilar-membrane nonlinearity estimated by pulsation threshold," J. Acoust. Soc. Am. **107**, 501–507.

Plack, C. J., Drga, V., and Lopez-Poveda, E. A. (**2004**). "Inferred basilar-membrane response functions for listeners with mild to moderate sensorineural hearing loss," J. Acoust. Soc. Am. **115**, 1684–1695.

Rhode, W. S., and Cooper, N. P. (**1996**). "Nonlinear mechanics in the apical turn of the chinchilla cochlea in vivo," Aud. Neurosci. **3**, 101–121.

Robles, L., and Ruggero, M. A. (**2001**). "Mechanics of the mammalian cochlea," Physiol. Rev. **81**, 1305–1352.

Rosengard, P. S., Oxenham, A. J., and Braida, L. D. (**2005**). "Comparing different estimates of compression in listeners with normal and impaired hearing," J. Acoust. Soc. Am. **117**, 3028–3041.

Shera, C. A., and Guinan, J. J., Jr. (**2008**). "Mechanisms of mammalian otoacoustic emissions," in *Active Processes and Otoacoustic Emissions*, edited by G. A. Manley, R. R. Fay, and A. N. Popper (Springer, New York), Chap. 9, pp. 305–342.

Stainsby, T. H., and Moore, B. C. J. (**2006**). "Temporal masking curves for hearing-impaired listeners," Hear. Res. **218**, 98–111.

Williams, E. J., and Bacon, S. P. (**2005**). "Compression estimates using behavioral and otoacoustic emission measures," Hear. Res. **201**, 44–54.

Wojtczak, M., and Oxenham, A. J. (**2009**). "Pitfalls in behavioral estimates of basilar-membrane compression in humans," J. Acoust. Soc. Am. **125**, 270–281.